CHEMBIOCHEM

DOI: 10.1002/cbic.200800538

The Molecular Basis of Inhibition of Golgi α-Mannosidase II by Mannostatin A

Douglas A. Kuntz,[a] Wei Zhong,[b] Jun Guo,[b] David R. Rose,*[a] and Geert-Jan Boons*[b]

Mannostatin A is a potent inhibitor of the mannose-trimming enzyme, Golgi α-mannosidase II (GMII), which acts late in the N*-glycan processing pathway. Inhibition of this enzyme provides a route to blocking the transformation-associated changes in cancer cell surface oligosaccharide structures. Here, we report on the synthesis of new Mannostatin derivatives and analyze their binding in the active site of* Drosophila *GMII by X-ray crystallography. The results indicate that the interaction with the backbone carbonyl of Arg876 is crucial to the high potency of the inhibitor—an effect enhanced by the hydrophobic interaction between the thiomethyl group and an aromatic pocket vicinal to the cleavage site. The various structures indicate that differences in the hydration of protein–ligand complexes are also important determinants of plasticity as well as selectivity of inhibitor binding.*

Introduction

Cells that have undergone oncogenic transformation often display abnormal cell surface oligosaccharides. These changes in glycosylation are important determinants of the stage, direction and fate of tumor progression. A potential route for blocking the changes in cell surface oligosaccharide structures is through inhibition of the mannose trimming enzyme Golgi α-mannosidase II (GMII; mannosyl-oligosaccharide 1,3-1,6-α-mannosidase II; E.C. 3.2.1.114), which acts late in the *N*-glycan processing pathway.[1,2] GMII acts on $GlcNAcMan_5GlcNAc_2$ to selectively cleave α(1-3) and α(1-6) mannosyl residues.[3,4]

Structural details of the substrate cleavage events have recently been elucidated by using the catalytic domain of the *Drosophila melanogaster* enzyme (dGMII).[5–7] GMII, a retaining family 38 glycoside hydrolase, employs a two-stage mechanism involving two carboxylic acids positioned within the active site, which act in concert; one acts as a catalytic nucleophile (Asp204 in dGMII) and the other as a general acid/base catalyst (Asp341 in dGMII). Protonation of the exocyclic glycosyl oxygen of a substrate molecule leads to bond breaking and simultaneous attack of the catalytic nucleophile to form a glycosyl enzyme intermediate.[5] Subsequent hydrolysis of the covalent intermediate by a nucleophilic water molecule gives an α-mannose product.

Mannostatins A (**1**) and B (**2**), which were isolated from the soil microorganism *Streptoverticillus*, were the first nonazasugar-type inhibitors to be discovered that possess an aminocyclopentitol structure, and are some of the most potent inhibitors of class II α-mannosidases reported (Figure 1).[8] The inhibitors are of the reversible, competitive type. Mannostatin A effectively blocked the processing of influenza viral hemagglutinin in cultured MDCK cells and caused the accumulation of hybrid-type protein linked oligosaccharides; this is consistent with blocking the action of Golgi mannosidase II.[9]

We previously reported an X-ray crystal structure of dGMII in complex with mannostatin A (**1**).[10] The five-membered ring of **1** adopts a $^2T_1$ twist envelope conformation, which is stacked against the aromatic ring of Trp95, and acts as a mimic of the covalently linked mannosyl intermediate. The 2,3-*cis*-diol (carbohydrate base numbering rather than strict IUPAC numbering is used here for comparative purposes) complexes with a Zn^{2+} ion in the active site of dGMII; this results in T_6 coordination geometry. Furthermore, the amine of **1** forms hydrogen bonds with catalytic acid residues Asp204, Asp341 and Tyr269. Data from SAR experiments have pointed to the importance of the amine and *cis*-diols for inhibitory activity of mannostatin A[11–18] and the crystal structure illustrated how these groups interact with the protein.

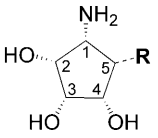

1 R = —SMe Mannostatin A K_i = 36 nM
2 R = —S(O)Me Mannostatin B K_i = 150 nM
3 R = —H K_i = 265 μM
4a R = —OH K_i = 300 nM
4b R = ⋯OH IC_{50} = 100 μM
5 R = —OMe K_i = 76 nM

Figure 1. Mannostatins A (**1**) and B (**2**) and analogues. The numbering scheme follows, as closely as possible, the carbohydrate numbering. Inhibition values for *Drosophila* Golgi α-mannosidase II are shown.

The thiomethyl moiety of **1**, which is structurally similar to the side chain of a methionine residue, is a feature that is not observed in any other glycosidase inhibitors. It has been proposed that the sulfur atom and ε-CH_3 (thiomethyl) group of

[a] *Dr. D. A. Kuntz,[+] Dr. D. R. Rose*
Ontario Cancer Institute and Department of Medical Biophysics
University of Toronto, Toronto, Ontario M5G 1L7 (Canada)
Fax: (+1) 416-581-7562
E-mail: drose@uhnresearch.ca

[b] *Dr. W. Zhong,[+] Dr. J. Guo, Dr. G.-J. Boons*
Complex Carbohydrate Research Center, University of Georgia
315 Riverbend Road, Athens, GA 30602 (USA)
Fax: (+1) 706-542-4412
E-mail: gjboons@ccrc.uga.edu

[+] *These authors contributed equally and should both be regarded as first authors.*

Supporting information for this article is available on the WWW under http://dx.doi.org/10.1002/cbic.200800538 or from the author.

methionine residues are involved in several different interactions important for protein stability.[19–22] The methyl carbon of the thiomethyl moiety of **1** in complex with dGMII appeared to adopt two different conformations.[10] In both conformations, the sulfur interacts with the backbone oxygen of Arg876 through the π orbital on the carbonyl oxygen and the antibonding σ* orbital of the S–C bond. In the cf1 conformation, the polarizable methyl group is in a hydrophilic environment and interacts with three water molecules and the π system of the Arg228 side chain. On the other hand, the methyl group of the cf2 conformation is in a hydrophobic pocket where it forms CH–π type interactions with the phenyl rings of Phe206 and Tyr727.

To probe the interactions of the thiomethyl function of **1** with dGMII in detail, mannostatin B (**2**) and analogues **3**, **4a**, **4b** and **5**, which contain deoxy, hydroxy, *epi*-hydroxy or methoxy substituents, respectively, instead of the thiomethyl of **1**, were prepared. The ability of the compounds to inhibit dGMII activity has been examined and the results rationalized by examining X-ray cocrystal structures of dGMII with the synthetic compounds. The results indicate that the previously observed dual conformations of the thiomethyl group might in fact have been an artifact of limited radiation damage, and the primary interaction of the methyl group is with the hydrophobic region of the cleavage pocket; this orients the sulfur such that its unpaired electrons make an interaction with the backbone carbonyl of Arg876, which seems to be a critical determinant of potency. The degree of penetrance of the methyl group into the hydrophobic site also appears to be important for the high potency of mannostatin A. Also, the various structures indicate that differences in the hydration of protein–ligand complexes are important determinant of plasticity as well as selectivity of inhibitor binding.

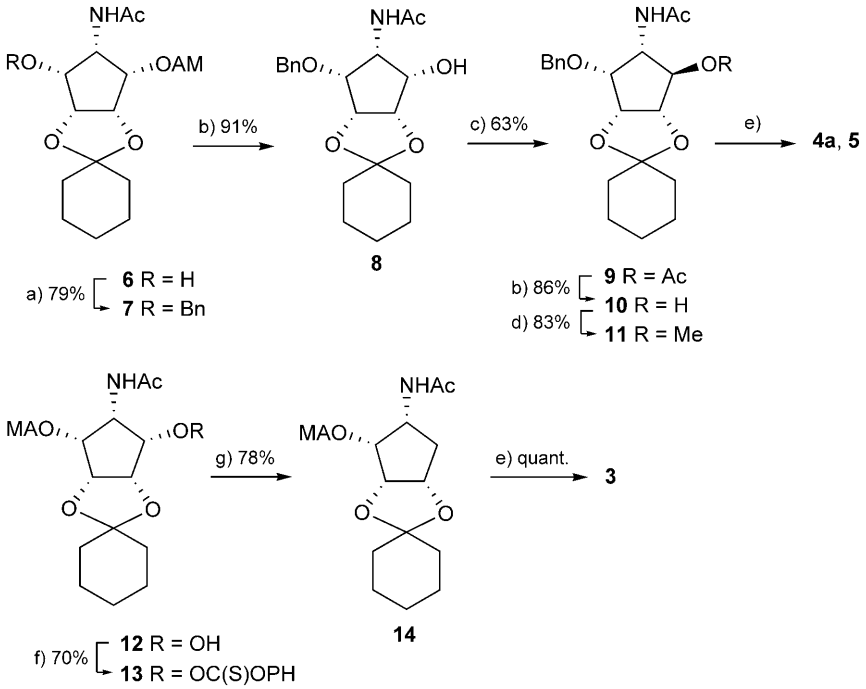

Scheme 1. Reagents and conditions: a) BnBr, Ag_2O, THF; b) NaOMe, MeOH; c) Tf_2O, Py, CH_2Cl_2, 0 °C then Bu_4NOAc, toluene; d) CH_3I, Ag_2O, CH_3CN; e) Pd/C, H_2, *t*BuOH, H_2O, AcOH then 1 M HCl in MeOH; f) phenylchlorothionoformate, DMAP, CH_3CN; g) Bu_3SnH, AIBN, toluene, Δ.

Results and Discussion

Chemical synthesis of mannostatin A analogues

Analogues **1**–**6** were synthesized to probe in detail the importance of the thiomethyl of substituents of mannostatin A for inhibiting GMII. Optically pure mannostatin A (**1**) and derivatives **6** and **12** were prepared by modified literature procedures.[11,15] The key steps of this approach were an aldol condensation of nitromethane with a dialdehyde derived from myo-inositol and a selective protection by an R-(−)-*O*-acetylmandelyl group. Thus, benzylation of **6** with benzyl bromide in the presence of silver(I) oxide in THF gave **7**, which was treated with NaOMe in methanol to remove the acetylmandelate (Am) ester to afford **8** (Scheme 1). Inversion of configuration of the C-2 hydroxyl of **8** was easily accomplished by triflation with triflic anhydride and pyridine in dichloromethane to give a triflate, which was immediately displaced by tetra-*n*-butylammonium acetate in toluene by using sonication to give acetate **9**. A small amount of elimination byproduct was also isolated. The acetyl ester of **9** was cleaved with sodium methoxide in methanol to afford **10**, which was methylated with methyl iodide in the presence of silver(I) oxide to give **11**. Deprotection of **10** and **11** to give the target compounds **4a** and **5** was accomplished by a two-step procedure involving catalytic hydrogenation over Pd/C to remove the benzyl ether followed by treatment with HCl (1 M) in a mixture of H_2O/MeOH to hydrolyze the cyclohexylidene acetal and convert the acetamido moiety into an amine.

Compound **3** could easily be prepared from **12** by treatment with DMAP and chlorothionoformate in acetonitrile to give phenylthiocarbonyl ester **13** (70%), which was deoxygenated by heating under reflux in the presence of the free radical initiator AIBN and reducing reagent tributyltin hydride in toluene to afford **14**. Deprotection of **14** was easily accomplished by heating under reflux in HCl (1 M) in H_2O/MeOH to give 5-deoxy-aminocyclopetititol **3**. Compound **4b** could be prepared by standard deprotection of **8**.

Enzymology

The rate of hydrolysis catalyzed by dGMII of different concentrations of 4-methylumbelliferyl α-D-mannopyranoside alone and in the presence of different concentrations of inhibitor was measured fluorometrically and K_i values were determined from Dixon plots. As can be seen in Figure 1, mannostatin A (**1**) is a more potent inhibitor than mannostatin B (**2**). 1-Deoxyaminocyclopentitetrol (**3**), which lacks the thiomethyl ether, is a very poor inhibitor; this indicates that the thiomethyl moiety of **1** makes important interactions with the binding site of the enzyme. Addition of the hydroxy group (**4a**) increases the potency by almost 1000-fold. The orientation of the hydroxy group was critical, as a downwardly oriented *epi*-hydroxyl (**4b**) only led to an approximate threefold increase in potency. Changing the hydroxyl of **4** to a methoxy group (**5**) further enhanced the potency by ~fourfold. However, the K_i values for **4a** and **5** were eight- and four-times larger than that of mannostatin A (**1**).

The thiomethyl group of mannostatin A interacts with the hydrophobic pocket

Analysis of X-ray crystal structure of dGMII–**1** complexes at various pH values (3.8, 5.75 and 9.0) by using the A1 line of the Cornell High Energy Synchrotron Source (CHESS) showed that the electron density of the ligand was divided into two discreet regions; the five-membered ring was separated from the thiomethyl group most likely as a result of radiation damage (Figure 2, top panel).

Because of their unique chemistries, active-site regions of enzymes are particularly prone to radiation-induced damage. It has been proposed that damaging species follow the electric field lines around proteins,[23] which could be expected to target the active site. In addition, sulfur and selenium containing amino acids are also usual targets, and the loss of thiomethyl groups of methionine[24] and methylseleno groups of selenomethione[23] have been reported. Furthermore, metalloenzymes are particularly sensitive to damaging effects of X-ray radiation.[25] Therefore, it is not surprising that the thiomethyl containing mannostatin A, which tightly bound in the zinc-containing active site, is susceptible to radiation-induced damage. We have previously not observed this damage in other complexes that contain selenium and sulfur containing inhibitors,[26,27] and it might have been exacerbated by the particularly high flux rates at the time of data collection. We did not observe the "split density" phenomenon with either mannostatin B (**2**) or the methyl ether analogue **5** (see below), and therefore it might be that the thiomethyl group is particularly prone to radiation damage. In any event, it made it impossible to assign any pH dependent conformation.

Data recollected with a rotating anode source with freshly prepared crystals did not show any evidence of radiation damage (Figure 2, lower panel). At all three pH values, the thiomethyl group was found in only one orientation: pointing towards the hydrophobic pocket formed by Phe206, Trp415 and Tyr727. We conclude that mannostatin A binds with its hydrophobic thiomethyl group in this aromatic pocket. Given the radiation damage we observed, it is probable that the previously observed dual conformation of the thiomethyl group might be a result of a limited amount of radiation damage. The orientation of mannostatin A with the thiomethyl pointing towards the hydrophobic pocket is in agreement with molecular dynamics studies.[10]

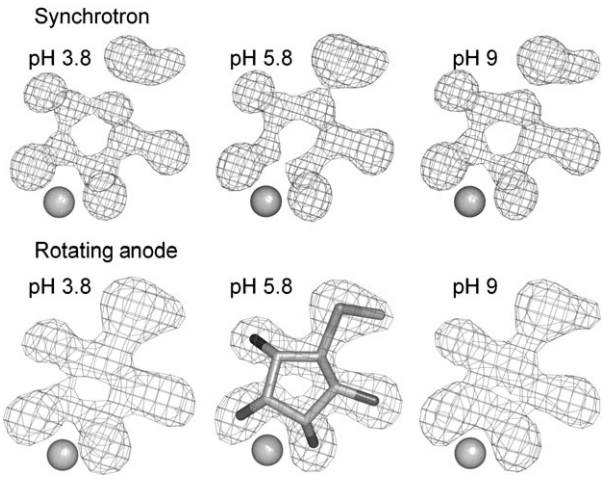

Figure 2. Radiation induced damage of mannostatin A bound in the active site of dGMII. The top row shows the electron density in the active site of dGMII–**1** crystals soaked at various pH values. The thiomethyl group is in a region of unusual shaped density and is separated from the ring. Data were collected by using the CHESS A1 line. Under similar conditions, on a rotating anode the density is intact and has the expected shape (lower panel). In each case the methyl group points towards the hydrophobic pocket and a second conformer is not observed. Fitted mannostatin A is shown in the pH 5.8 electron density. The active site zinc is shown as a gray sphere.

Cocrystal structures of dGMII with compounds 2–5

Crystallographic analysis of dGMII was carried out with the five mannostatin analogues (**2**–**5**), either prepared as cocrystals or by soaking of crystals previously washed with phosphate buffer (to remove bound Tris arising from the crystallization solution). Data collection was performed on a rotating anode or with synchrotron radiation. Structural refinement was carried out to a final resolution ranging from 1.21 to 1.85 Å with *R* values in the range of 0.13 to 0.19. Details of data collection and refinement statistics are provided in Table S1 in the Supporting Information. Simulated annealing F_o-F_c omit maps are presented in Figure 3. Stereoviews of the electron density for each compound are provided in the Supporting Information (Figure S1). The density for the ring apposing the active-site zinc is exceptionally clear in all complexes, a result reflected in the low temperature factors ("B factors" 8–15 Å^2) of this ring. These low B factors are consistent with the many tight interactions made between the inhibitor and the active site amino acids and, especially, the active site zinc.

Details of the binding of one of the analogues (mannostatin B) in the active (−1) site of dGMII are shown in Figure 4. Trp95 forms the roof of the active-site pocket and makes a stacking interaction with the five-membered ring. The thio-

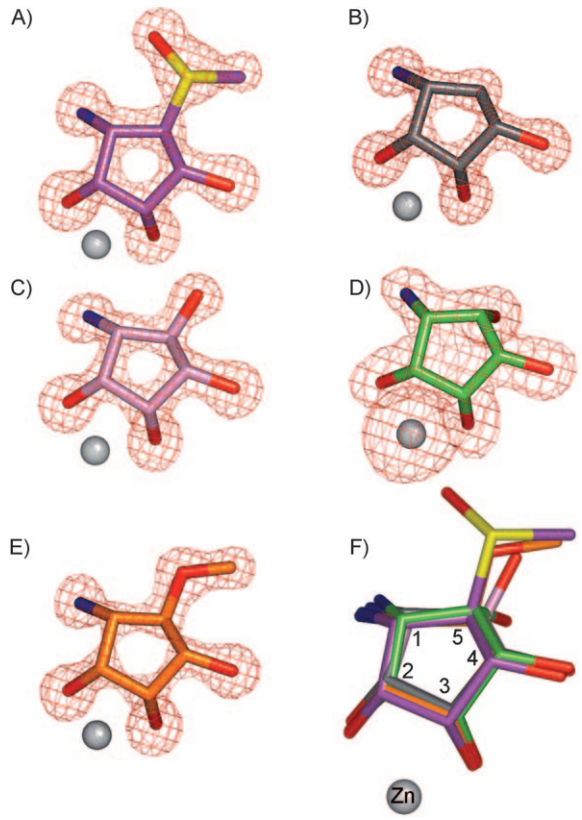

Figure 3. Bound compounds in the active site of dGMII. Simulated annealing (3000 K) F_o-F_c omit maps were generated in CNS.[38] The electron density was contoured at 5σ. In all cases the compound was removed from the final model before generation of the omit maps. A) Compound **2** (mannostatin B); B) compound **3**; C) compound **4a**; D) compound **4b**; here the zinc was also removed; E) compound **5**. Stereoviews of all of these complexes are shown in Figure S1. F) Coordinates for all structures reported here were superimposed, by using the SSM subroutine in Coot.[39] The colors match the density diagrams: mannostatin B is magenta, **3** is gray, **4a** is pink, **4b** is green, and **5** is orange.

methyl group resides in a hydrophobic region consisting of Phe206, Trp415 and Tyr727. Atoms closely interacting (distance <3.2 Å), including through hydrogen bonds and electrostatic interactions, are detailed in Figure 5B. Predominant tight interactions are formed between the O2 and O3 of the inhibitor and the zinc ion. These interactions have a similar distance (2.1–2.2 Å) and presumably similar strength, to the interactions made with the amino acids of dGMII that tightly hold the zinc in the protein. Other interactions, which have previously been shown by molecular dynamic simulations[10] to be particularly important for mannostatin A binding, include those with Asp472, Asp341 and Tyr269. The distance between the Asp341 Oδ2 and the O2 has lengthened to 3.3 Å and does not show up in the interaction diagram. The catalytic nucleophile Asp204 Oδ2 makes interactions with both O2 and the amino group. The amino group, in turn, is involved in other interactions including ones with the acid/base catalyst Asp341, Tyr269-OH and a water molecule. The unique oxygen of the sulfoxide moiety of mannostatin B makes contacts with two waters (one which interacts with both Tyr269-OH and the amino group, the other interacts with the backbone carbonyl of Arg876) and the NH_2 group of Arg228.

A superposition of compounds **1**–**5** is shown in Figure 3F, which clearly demonstrates they bind at nearly identical positions and adopt very similar conformations. Interaction diagrams, provided in Figure 5 indicate that there is very little difference in the interaction distances in the various mannostatin–analogue complexes. The addition of a hydroxyl to compound **3** resulted in new interactions with the protein; Arg228 NH_2 makes a new hydrogen bond with the OH of both **4a** and **4b**. Compound **4b** also makes new close interactions with both Asp204 Oδ1 and Oδ2, similar to what was seen in the dGMII–mannose structure (Figure S2). However, despite these new interactions, **4b** is only slightly (~threefold) more potent than **3**; this indicates that these interactions are not principle determinants of tight binding. Thus, the configuration of the substituent at the C-5 is critical for high affinity binding, with the upward configuration (as in **4a**) being the active one. For the other compounds, the principal changes cluster around the amino group, and the interactions made with Asp341. The least potent compounds (**3**, **4a**, **4b**) lack a close interaction between the amino group on the five-membered ring and the Oδ2 of the acid/base catalyst Asp341 (the distances have extended to 3.4–3.6 Å) and instead the closest interaction is mediated by a water molecule (Figures 5C–E). This is a relatively high B factor water molecule, which is not present in the structures with the other analogues. The presence of this intermediate water and the increase in hydrogen bond lengths presumably weakens the strength of the interaction between the compounds and the protein. We have recently shown that interactions between Asp341 and a properly positioned amino group are important for greatly enhancing the potency of kifunensine-like inhibitors,[28] especially if the nitrogen is positively charged. This, however, does provide an explanation of the ~4000-fold difference in potencies between **1** (Figure 5A) and **3** (Figure 5C). Also, **4a** (Figure 5D) is a ~1000-fold better inhibitor than **3**, but the binding geometry to the amino substituent is nearly identical, so the difference must be mediated by the upwardly oriented substituent at C-5.

The role of the C-5 substituent of the mannostatin analogues for inhibitory activity

The mannostatin analogues, which only differ in the substituent attached to C-5, are positioned in the same way in the active site of dGMII (Figure 3F), and with the exception of the C-5 substituent make nearly identical interactions with the protein (Figure 5). This indicates that the nearly 7500-fold difference in inhibitory potency between the unsubstituted **3** and mannostatin A (**1**) must arise from differences in interactions of the C-5 substituents, which result in changes in the active-site hydration, formation of hydrogen bonds and apolar contacts. The increasingly complex nature of the substituents added at C-5 allows us to dissect these various effects.

1) *Changes in water structure mediated by analogue binding.* As mentioned above, a nearly three-orders of magnitude in-

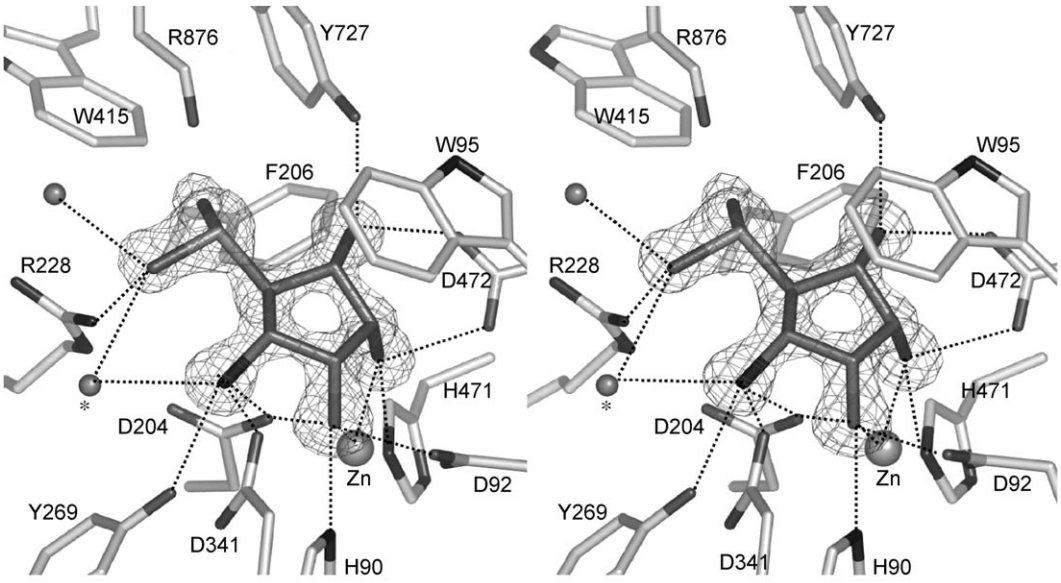

Figure 4. Binding of mannostatin B (**2**) in the active site of dGMII. Divergent stereoview of mannostatin B (dark gray) showing important interacting dGMII residues (light gray). Close interactions (< 3.2 Å) are shown as dotted lines and have lengths as shown in Figure 5B. The simulated annealing (3000 K) F_o-F_c omit electron density map was generated in CNS[38] and is contoured at 5σ. The active site zinc is indicated as a large sphere and waters are represented as smaller spheres. The asterisk indicates the position of the water that is common in all structures, and which forms an additional interaction with either R228-NH_2 or Y269-OH.

crease in inhibitory potency of **3** results from addition of a properly oriented hydroxyl at C-5 to give **4a.** Although **3** and **4a** only differ by a single hydroxyl residue there is nearly three-orders of magnitude difference in inhibitory potency (Figure 1). A superposition of dGMII–**3** and dGMII–**4a** is presented in Figure 6A. The positions of the bound inhibitors are identical as are the positions of the amino acids in the active site, with the exception of a small movement in the peptide backbone around Arg876. The major variation is in the positions of the water molecules. Movement of a single water molecule, which allows a water-mediated interaction to form between the backbone carbonyl of Arg876 (Arg876O) and the novel hydroxyl of **4a** (Figure 5D), appears to cause a cascade of water rearrangement in the active site (Figure 6A). The rearrangement results in loss of a water molecule seen in the dGMII–**3** structure (indicated by an asterisk in Figure 6A) which is also present in the structure with the poor inhibitor **4b**. Thus, the presence of this water seems to correlate with poor inhibitory potential. This water residue makes hydrogen bonds to Asp204 Oδ1 and Arg228 Nε and could reduce the strength of the hydrogen bonds made between these two residues and the inhibitors.

Well-resolved water molecules, which are often observed in carbohydrate–protein complexes, can contribute to the specificity as well as to plasticity of ligand recognition. For example, crystallographic studies of the binding specificities of the bacterial L-arabinose binding protein (ABP) have shown that an order of a magnitude higher affinity of L-arabinose compared to D-fucose are due to differences in hydration of the carbohydrate–protein complexes.[29] The higher affinity of binding of L-arabinose was attributed to the presence of two water molecules that filled a potential gap between protein and ligand. Furthermore, the relative high affinity of D-galactose for ABP was attributed to displacement of a water molecule by the C-6 hydroxymethyl. Previously, we have shown that water rearrangement can have a dramatic influence on inhibitor potency. In studies with swainsonine-type derivatives, the addition of a single hydroxyl caused a sufficient side-chain movement of Arg228 to dislodge a conserved water; this leads to disruption of the water structure and results in a significant loss (> 130-fold) of inhibitor potency[27] against dGMII. However, in the structures studied here, the waters in question are not tightly bound (B factors > 25 Å^2) and are located at the edge of the binding pocket, and the effect might be due to the Arg876O interaction (discussed below) and changes in hydrogen bond strength (discussed above) rather than the water rearrangement per se, although all components might contribute.

2) *Interaction with the backbone carbonyl of Arginine 876.* Arg876O has been implicated in binding a large number of compounds to dGMII, although many of them are weak inhibitors. Arg876O interacts directly with the C-6 hydroxyl group of the natural substrate,[6,7] and direct interactions are also observed with a number of inhibitors including deoxymannojirimycin,[30] kifunensine,[31] salacinol analogues,[26,32] and manno-noeuromycin.[33] Water mediated interactions with Arg876O have also been observed with pyrrolidine-based inhibitors.[34,35]

The water-mediated interaction between the C-5 hydroxyl of **4a**, which results in a ~300-fold increase in potency compared to *epi* substituted **4b**, argues for the importance of the Arg876O interaction for binding mannostatin ana-

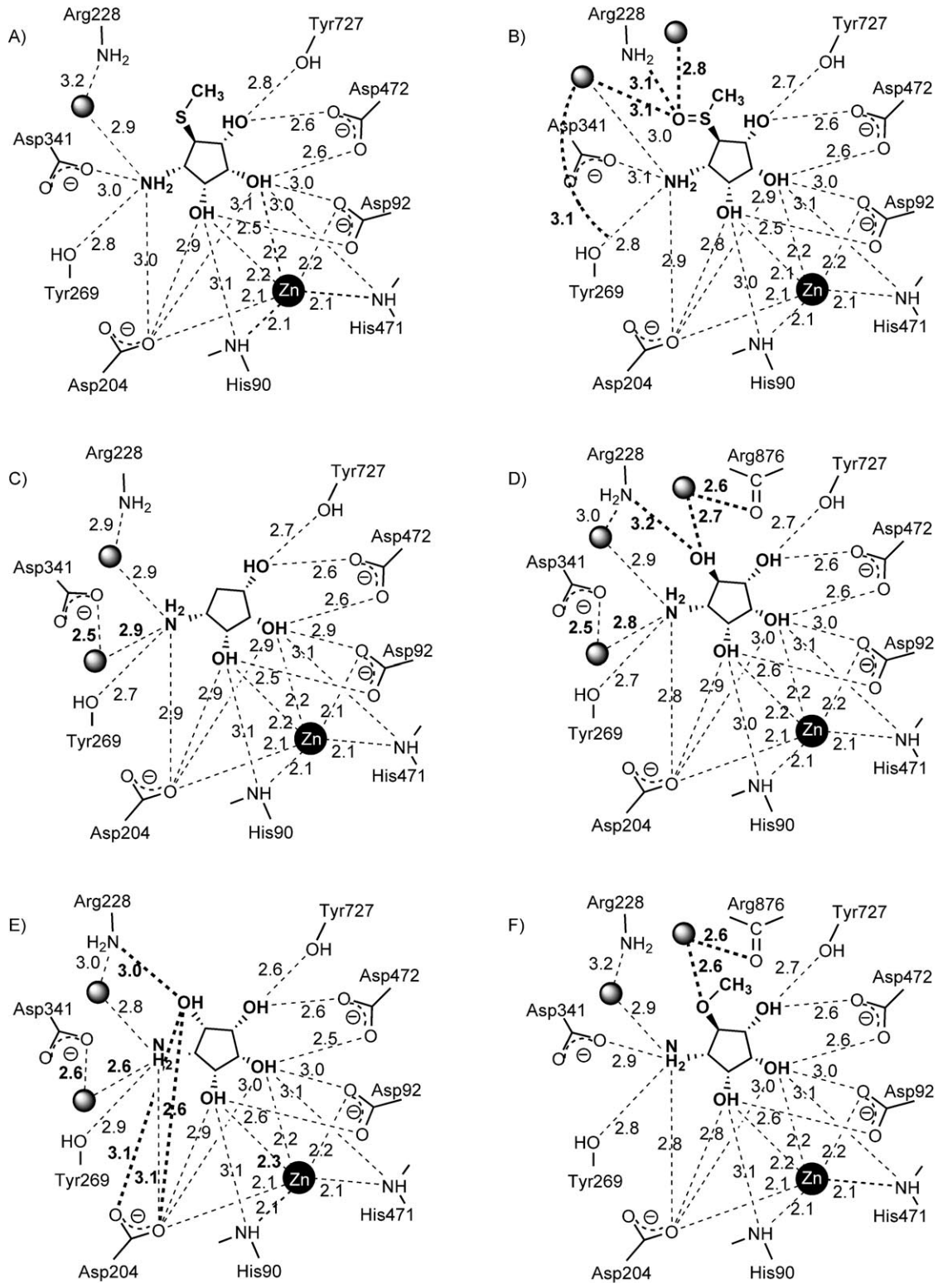

Figure 5. Tight interactions (3.2 Å or less) of the bound compounds in the active site of dGMII. A) Mannostatin A at pH 5.75; B) mannostatin B; C) compound **3**; D) compound **4a**; E) compound **4b**; F) compound **5**. All distances are given in Ångström units. Water molecules are shown as gray spheres and the zinc is shown as a black sphere. Interactions that change significantly from mannostatin A are shown in bold. New interactions not seen in A) are shown as thicker dotted lines with distances listed in bold.

logues. A comparison of **4a** with the strongest inhibitor, mannostatin A, is shown in Figure 6B. The water forming the through-water interaction with Arg876O has been displaced by 1.9 Å and Arg876O makes a direct interaction (3.8 Å) with the sulfur. The Arg876O–S interaction, which is unique for the complex of dGMII with **1**, could significantly

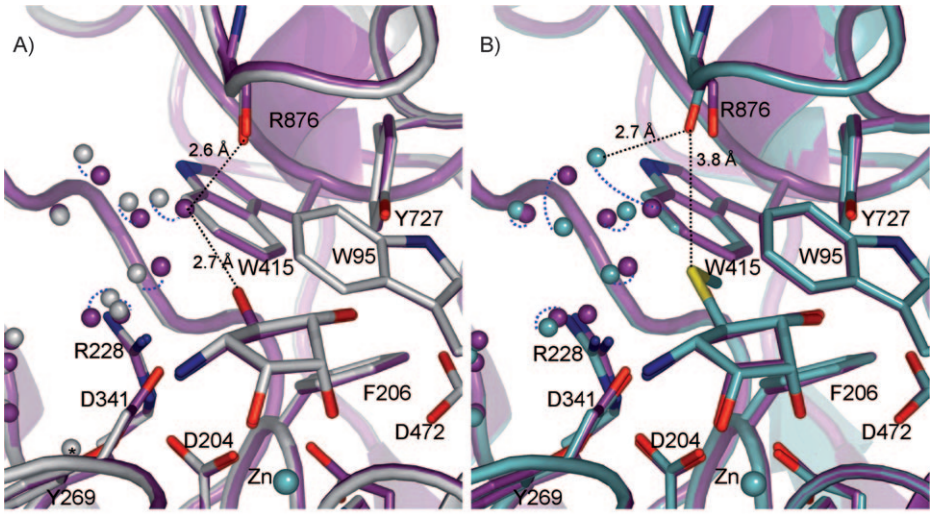

Figure 6. Interactions of mannostatin analogues with the backbone carbonyl of Arg876: comparison of the active-site environment of two inhibitors differing in potency by three orders of magnitude. A) The active site of dGMII–**3** (white, $K_i = 265$ μM) and dGMII–**4a** (magenta, $K_i = 300$ nM). The newly formed through-water interaction between the hydroxyl group of **4a** and the backbone carbonyl of Arg876 of dGMII is shown as a black dotted line. Comparable waters are shown joined by a blue dotted arc. The asterisk indicates the position of a water molecule that is present only in dGMII–**3**. B) The active site of dGMII–**4a** (magenta, $K_i = 300$ nM) and dGMII–**1** (cyan, $K_i = 38$ nM) collected at pH 5.75. Superpositions were carried out with Coot.[39]

contribute to binding. The sulfur of methionine residues and backbone carbonyl oxygens or side chain carboxylate oxygen often make S–O type interactions, with the interaction occurring between the π orbital on the carbonyl oxygen and the antibonding σ* orbital of S–C bond.[22] At a distance 3.3 Å these interactions could result in stabilization of up to 2.5 kcal mol^{-1} as modeled by ab initio calculations.[22] In the dGMII–**1** complex the sulfur atom is located at 3.8 Å from Arg876O; this suggests a reasonably strong interaction. A strong interaction also provides an explanation for the shape of the electron density observed in structures that experienced radiation damage and resulted in cleavage of the thiomethyl group, which moved towards the Arg876O giving an appearance of a second conformation.

3) *Interactions with the aromatic pocket of the active site.* Hydrophobic interactions with the aromatic region of the active site (consisting of conserved residues Phe206, Trp415 and Tyr727) are also important in the binding of several inhibitors to dGMII. In the case of swainsonine ($K_i = 20$ nM), Arg876O does not seem to play a role in complexation, but rather there is an interaction with the hydrophobic region of the active site. Furthermore, it was recently demonstrated that the addition of a methyl group to a pyrrolidine based inhibitor, which led to both a loss of the water-mediated Arg876O interaction and the formation of a new hydrophobic interaction with the aromatic region, resulted in a K_i reduced by over 20-fold.[34]

Interactions between the aromatic region of the dGMII active site and the methyl group of the mannostatin analogues are shown in Figure 7 and compared with those formed with swainsonine. In the case of swainsonine, the interactions are formed with a six-membered ring rather than a simple methyl group and therefore are expected to be stronger (Figure 7D). The shortest range interactions in the dGMII–swainsonine complex are between the inhibitor and Tyr727 and Phe206. The closest interactions made by the mannostatin analogues are with the end of the Trp415 ring where the methyl group is positioned equidistant between the CH_2 and CZ3 carbons. Mannostatin A, which is best inhibitor among the analogues, demonstrates the shortest distances to Phe206, which could be a key determinant of potency. The methyl group of mannostatin A is centrally spaced

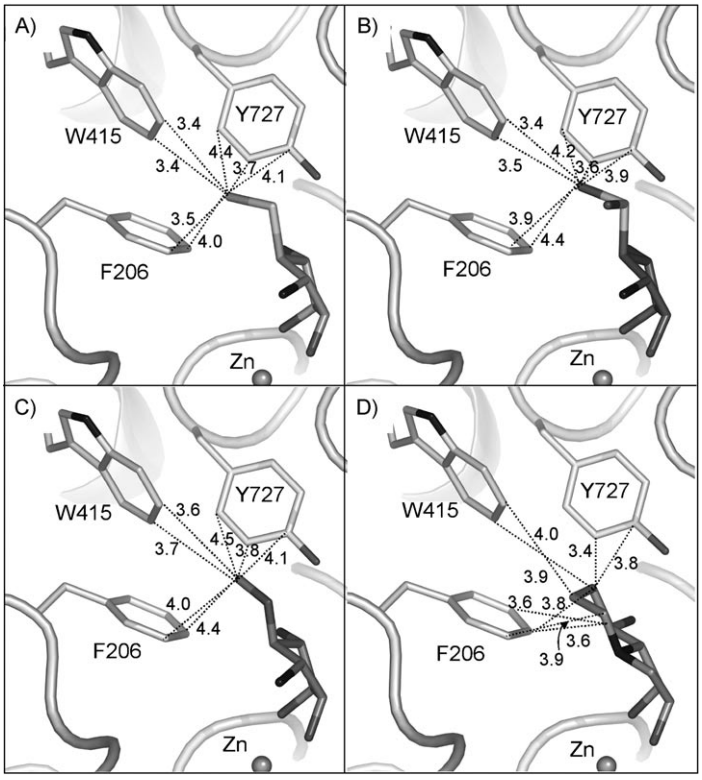

Figure 7. Hydrophobic interactions between dGMII and bound inhibitors. Interaction distances between residues of the aromatic cluster of dGMII and hydrophobic regions of the inhibitors are indicated (in Ångström units). A) Mannostatin A (pH 5.75 structure), B) mannostatin B, C) compound **5**, D) swainsonine (PDB ID: 3BLB).

with respect to the centroid of the aromatic rings at distances from the methyl carbon of 4.4 Å for Phe206, 4.6 Å for Trp415, and 4.5 Å for Tyr737. In the case of mannostatin B, interactions of the sulfinyl group with a water molecule (as shown in Figure 4) appear to have pulled the methyl away from Phe206 and reduced its interaction. The hydroxymethyl group of **5** does not extend as far as the thiomethyl group of mannostatin A into the hydrophobic pocket, which could contribute to the somewhat lower inhibitory activity of this compound.

Mannostatin B (**2**), the hydroxy containing derivative **4a**, and methyl ether containing derivative **5** make interactions with the protein that are not observed in the complex with **1**, and might compensate for a loss of some of the interactions observed in the complex with **1**. For example, mannostatin B (**2**), which has only a fourfold reduction in potency compared to **1**, makes unique interactions through the oxygen of the sulfoxide moiety with the NH_2 group of Arg228 and two waters. The hydroxyl of **4a** also makes a hydrogen bond with Arg228 NH_2, but since a similarly distanced interaction occurs in the 100 μM inhibitor **4b** (Figure 5E) this bond is not expected to contribute significantly. Furthermore, oxygen of the methyl ether of the **5** makes a hydrogen bond with a water molecule, which in turn interacts with the main chain carbonyl oxygen of Arg876.

Conclusions

Through a combined use of synthetic chemistry, enzymology and X-ray crystallography, the catalytic site of dGMII has been studied in detail. The relatively large number of inhibitors employed and the high resolution of the crystallographic structures provided a unique opportunity to dissect the determinants of inhibitor activity at the level of different substituents introduced at different ring positions. The analysis is not only at the level of inhibitory potency, but also includes the visualization of the atomic basis for the effects. Specifically, our previous studies have pointed to the crucial contribution of zinc interactions, and interactions with Asp341 and Asp472, as well as the importance of water structure in inhibitor binding. The data presented here illustrate the importance of the interaction of the Arg876 backbone carbonyl as well as hydrophobic interactions with Phe206, Trp415 and Tyr727 as additional contributory factors. Furthermore, analyses of the various structures indicate that differences in the hydration of the protein binding site, is an important factor for plasticity as well as selectivity of inhibitor binding. In retrospect, it is not surprising that the active site of GMII has proven difficult to model accurately,[35,36] since small differences in inhibitor chemistry result in large differences in inhibitor potency.

Experimental Section

Synthesis procedures

General experimental procedures: Chemicals were purchased from Aldrich or Fluka and used without further purification. DCM was distilled from calcium hydride; THF from sodium; and MeOH from magnesium and iodine. Aqueous solutions are saturated unless otherwise specified. All reactions were performed under anhydrous conditions under argon unless otherwise specified and monitored by TLC on Kieselgel 60 F254 (Merck). Detection was carried out by examination under UV light (254 nm) and by charring with sulfuric acid (10%) in methanol. Silica gel (Merck, 70-230 mesh) was used for chromatographies. Iatrobeads 6RS-8060 was purchased from Bioscan.

The ^{1}H NMR spectra were recorded either in $CDCl_3$ or D_2O by using a Varian Merc-300 or Varian Inova-500 spectrometers equipped with Sun workstations at 300 K. TMS ($\delta_H = 0.00$) or D_2O ($\delta_H = 4.67$) was used as the internal reference. The ^{13}C NMR spectra were recorded either in $CDCl_3$ or D_2O at 75 MHz on a Varian Merc-300 spectrometer, by using the central resonance of $CDCl_3$ ($\delta_C = 77.0$) as the internal reference. COSY, HSQC and NOSEY experiments were used to assist assignment of the products. Mass spectra were obtained by using an Applied Biosystems Voyager DE-Pro MALDI-TOF.

*(1S,2S,3R,4R,5R)-5-Acetamido-1-O-[(2R)-2-O-acetylmandelyl]-4-O-benzyl-1,2,3,4-cyclopentanetetrol (**7**)*: Benzyl bromide (0.16 mL, 1.34 mmol) and silver(I) oxide (1.55 g, 6.68 mmol) were added to a solution of **6** (0.30 g, 0.67 mmol) in THF (10 mL). The flask was wrapped in aluminium foil to exclude light and the reaction mixture stirred at room temperature for 24 h, after which it was filtered through celite. The filtrate was concentrated to dryness, and purification of the crude product by column chromatography (toluene/acetone, 3:1, *v/v*) on silica gel afforded **7** (0.285 g, 79%) as colorless oil; $R_f = 0.46$ (toluene/acetone, 3:1, *v/v*); ^{1}H NMR (300 MHz, $CDCl_3$): $\delta = 7.40$–7.09 (m, 10H, Ph), 5.96 (s, 1H, PhC*H*(OAc)CO), 5.93 (d, $J_{5,NH} = 8.1$ Hz, 1H, NH), 4.70 (dd, $J_{1,2} = 5.4$ Hz, $J_{1,5} = 5.4$ Hz, 1H, H-1), 4.64 (ddd, $J_{1,5} = 5.4$ Hz, $J_{4,5} = 4.8$ Hz, 1H, H-5), 4.59–4.49 (m, 4H, H-2, H-3, PhCH_2), 3.60 (t, $J_{3,4} = 4.8$ Hz, $J_{4,5} = 4.8$ Hz, 1H, H-4), 2.11 (s, 3H, PhCH(CH_3CO)CO), 1.86 (s, 3H, CH_3CONH), 1.72–1.32 (m, 10H, C_6H_{10}) ppm; ^{13}C NMR (75 MHz, $CDCl_3$): $\delta = 170.3$, 169.3, 167.7 (*C*=O), 137.4–127.8 (C_{arom}), 113.4(C_6H_{10}), 79.1 (C-2), 77.2 (C-3), 74.2 (C-4), 74.1 (Ph*C*H(OAc)CO), 72.3 (Ph*C*H_2), 71.7 (C-1), 49.9 (C-5), [35.9, 33.2, 25.0, 24.0, 23.4 (C_6H_{10})], 23.1 (*C*H_3CONH), 20.7 (PhCH(*C*H_3CO)CO); HRMS: *m/z*: found $[M+Na]^+$ 560.2257, $C_{30}H_{35}NO_8$ calcd for $[M+Na]^+$ 560.2260.

*(1S,2S,3R,4R,5R)-5-Acetamido-4-O-benzyl-1,2,3,4-cyclopentanetetraol (**8**)*: NaOMe was added to a solution of **7** (0.28 g, 0.52 mmol) in MeOH/DCM (10 mL, 1:1, *v/v*) until a pH 9–10 was reached. The reaction mixture was stirred at room temperature for 18 h, and then neutralized by the addition of Dowex 650 H^+. The suspension was filtered through celite and the residue washed with MeOH/DCM (10 mL, 1:1, *v/v*). The combined filtrates were concentrated to dryness and purification of the residue by column chromatography (toluene/acetone, 3:1, *v/v*) on silica gel afforded **8** (0.17 g, 91%) as a colorless oil; $R_f = 0.17$ (toluene/acetone, 2:1, *v/v*); ^{1}H NMR (300 MHz, $CDCl_3$): $\delta = 7.27$–7.19 (m, 5H, Ph), 6.29 (d, $J_{5,NH} = 8.1$ Hz, 1H, NH), 4.62–4.52 (m, 3H, H-2, PhCH_2), 4.45 (t, $J_{2,3} = 6.0$ Hz, $J_{3,4} = 5.7$ Hz, 1H, H-3), 4.37 (ddd, $J_{1,5} = 4.8$ Hz, $J_{4,5} = 5.4$ Hz, 1H, H-5), 3.89 (t, $J_{3,4} = 5.7$ Hz, $J_{4,5} = 5.4$ Hz, 1H, H-4), 3.68 (t, $J_{1,2} = 4.5$ Hz, $J_{1,5} = 4.8$ Hz, 1H, H-1), 1.96 (s, 3H, CH_3CONH), 1.70–1.38 (m, 10H, C_6H_{10}); ^{13}C NMR (75 MHz, $CDCl_3$): $\delta = 170.4$ (*C*=O), 137.4–127.9 (C_{arom}), 113.4(C_6H_{10}), 79.4 (C-2), 77.2 (C-3), 75.2 (C-1), 72.6 (Ph*C*H_2), 70.7 (C-4), 52.6 (C-5), [35.8, 33.2, 25.0, 24.0, 23.4 (C_6H_{10})], 23.3 (*C*H_3CONH); HRMS: *m/z*: found $[M+Na]^+$ 384.1714, $C_{20}H_{27}NO_5$ calcd for $[M+Na]^+$ 384.1717.

*(1R,2S,3R,4R,5S)-5-Acetamido-1-O-acetyl-4-O-benzyl-1,2,3,4-cyclopentanetetraol (**9**)*: Trifluoromethanesulfonic anhydride (0.12 mL, 0.71 mmol) was added drop wise to a solution of **8** (0.17 g, 0.47 mmol) in pyridine (0.19 mL, 2.33 mmol) and DCM (5 mL) at 0 °C. The reaction mixture was stirred at 0 °C for 1 h, and then diluted with DCM (25 mL). The solution was washed with H_2O (10 mL) and saturated $NaHCO_3$ (10 mL). The organic layer was dried ($MgSO_4$), filtered and the filtrate concentrated to dryness. To a solution of this residue in toluene (20 mL) was added tetra-*n*-butylammonium acetate (0.28 g, 0.92 mmol). The reaction mixture was sonicated at room temperature for 18 h, and then concentrated under reduced pressure. The residue was dissolved in DCM (25 mL), and washed with saturated $NaHCO_3$ (10 mL) and brine (10 mL). The organic layer was dried ($MgSO_4$), filtered and the filtrate concentrated to dryness. Purification of the crude product by column chromatography on silica gel (toluene/acetone, 2:1, *v/v*) afforded **9** (0.12 g, 63%) as a colorless oil; R_f 0.42 (toluene/acetone, 2:1, *v/v*); ^{1}H NMR (300 MHz, $CDCl_3$): δ = 7.31–7.24 (m, 5H, Ph), 6.27 (d, $J_{5,NH}$ = 8.1 Hz, 1H, NH), 4.98 (d, $J_{1,5}$ = 2.4 Hz, 1H, H-1), 4.62–4.53 (m, 3H, H-3, PhCH_2), 4.37 (ddd, $J_{1,5}$ = 2.4 Hz, $J_{4,5}$ = 5.7 Hz, 1H, H-5), 4.32 (d, $J_{2,3}$ = 6.0 Hz, 1H, H-2), 3.93 (t, $J_{3,4}$ = 5.4 Hz, $J_{4,5}$ = 5.7 Hz, 1H, H-4), 1.96 (s, 3H, CH_3CO), 1.89 (s, 3H, CH_3CONH), 1.72–1.30 (m, 10H, C_6H_{10}); ^{13}C NMR (75 MHz, $CDCl_3$): δ = 170.4, 169.6 (*C*=O), 137.4–128.0 (C_{arom}), 113.3(C_6H_{10}), 81.9 (C-2), 79.3 (C-1), 78.8 (C-3), 76.6 (C-4), 72.5 (PhCH_2), 54.3 (C-5), [35.9, 33.1, 25.0, 23.8, 23.4 (C_6H_{10})], 23.3 (CH_3CONH), 20.9 (CH_3CO); HRMS: *m/z*: found $[M+Na]^+$ 403.1992, $C_{22}H_{29}NO_6$ calcd for $[M+Na]^+$ 403.1995.

*2,3-O-Cyclohexylidene derivative **10** of respective (1R,2S,3R,4R,5R)-5-acetamido-4-O-benzyl-1,2,3,4-cyclopentanetetrol (**10**)*: NaOMe was added to a solution of **9** (0.12 g, 0.30 mmol) in MeOH/DCM (1:1) until a of pH 9–10 was reached. The reaction mixture was stirred at room temperature for 18 h, and then neutralized by the addition of Dowex 650 H^+. The solution was filtered through celite, and the residue washed with MeOH/DCM (6 mL, 1:1, *v/v*). The combined filtrates were concentrated to dryness and purification of the residue by column chromatography (toluene/acetone, 2:1, *v/v*) on silica gel afforded **9** (0.092 g, 86%) as a colorless oil; R_f = 0.30 (toluene/acetone, 2:1, *v/v*); ^{1}H NMR (300 MHz, $CDCl_3$): δ = 7.28–7.09 (m, 5H, Ph), 6.39 (d, $J_{5,NH}$ = 6.3 Hz, 1H, NH), 4.64 (t, $J_{2,3}$ = 5.1 Hz, $J_{3,4}$ = 4.5 Hz, 1H, H-3), 4.56 (dd, 2H, J = 12 Hz, PhCH_2), 4.32 (d, $J_{2,3}$ = 5.1 Hz, 1H, H-2), 4.16 (ddd, $J_{1,5}$ = 1.5 Hz, $J_{4,5}$ = 4.5 Hz, 1H, H-5), 4.06 (t, $J_{3,4}$ = 4.5 Hz, $J_{4,5}$ = 4.5 Hz, 1H, H-4), 4.03 (d, $J_{1,5}$ = 1.5 Hz, 1H, H-1), 1.89 (s, 3H, CH_3CONH), 1.68–1.28 (m, 10H, C_6H_{10}); ^{13}C NMR (75 MHz, $CDCl_3$): δ = 170.4 (*C*=O), 137.4–128.1 (C_{arom}), 112.5(C_6H_{10}), 84.1 (C-2), 79.1 (C-3), 78.1 (C-1), 76.7 (C-4), 72.3 (PhCH_2), 57.6 (C-5), [35.9, 32.9, 25.1, 23.9, 23.4 (C_6H_{10})], 23.3 (CH_3CONH); HRMS: *m/z*: found $[M+Na]^+$ 384.1714, $C_{20}H_{27}NO_5$ calcd for $[M+Na]^+$ 384.1717.

*(1R,2S,3R,4R,5R)-5-Acetamido-4-O-benzyl-1-O-methyl-1,2,3,4-cyclopentanetetrol (**11**)*: Methyl iodide (52 μL, 0.84 mmol) and silver(I) oxide (0.16 g, 0.69 mmol) were added to a solution of **10** (50 mg, 0.14 mmol) in acetonitrile (2 mL). The flask was wrapped by aluminium foil to exclude light. The reaction mixture was stirred at room temperature for 48 h, and then filtered through celite. The filtrate was concentrated to dryness and purification of the residue by column chromatography (toluene/acetone, 3:1, *v/v*) on silica gel afforded **11** (43 mg, 83%) as a colorless oil; R_f = 0.45 (toluene/acetone, 2:1, *v/v*); ^{1}H NMR (300 MHz, $CDCl_3$): δ = 7.28–7.19 (m, 5H, Ph), 6.32 (d, $J_{5,NH}$ = 5.1 Hz, 1H, NH), 4.60–4.48 (m, 3H, H-3, PhCH_2), 4.30 (m, 2H, H-2, H-5), 3.93 (t, $J_{3,4}$ = 4.5 Hz, $J_{4,5}$ = 4.5 Hz, 1H, H-4), 3.54 (d, $J_{1,5}$ = 1.5 Hz, 1H, H-1), 3.34 (s, 3H, OCH_3), 1.90 (s, 3H, CH_3CONH), 1.69–1.28 (m, 10H, C_6H_{10}); ^{13}C NMR (75 MHz, $CDCl_3$): δ = 169.5 (*C*=O), 137.3–128.0 (C_{arom}), 112.5 (C_6H_{10}), 86.9 (C-2), 82.0 (C-3), 79.1 (C-1), 76.6 (C-4), 72.1 (PhCH_2), 57.6 (C-5), 53.5 (OCH_3), [36.0, 32.8, 25.0, 23.9, 23.4 (C_6H_{10})], 23.3 (CH_3CONH); HRMS: *m/z*: found $[M+Na]^+$ 375.2041, $C_{21}H_{29}NO_5$ calcd for $[M+Na]^+$ 375.2046.

*(1S,2S,3R,4R)-4-Acetamido-3-O-[(2R)-2-O-acetylmandelyl]-5-deoxy-1,2,3-cyclopentanetriol (**14**)*: DMAP (98 mg, 0.8 mmol) and phenyl chlorothionoformate (0.1 mL, 0.72 mmol) were added to a solution of **12** (60 mg, 0.13 mmol) in acetonitrile (0.6 mL). The mixture was stirred for 3 h at room temperature. After dilution with ethyl acetate (10 mL), the solution was washed with water (5 mL), dried ($MgSO_4$), filtered and the filtrate concentrated under reduced pressure. Purification of the residue by column chromatography (toluene/acetone, 3:1, *v/v*) on silica gel afforded the desired product **13** (55 mg, 79%) as a colorless oil; R_f = 0.7 (toluene/acetone, 1:1, *v/v*). A solution of **13** (44 mg, 0.08 mmol) in toluene (4 mL) was added to a solution of AIBN (4 mg, 0.023 mmol) and tributyltin hydride (60 μL, 0.23 mmol) in toluene (0.55 mL). The mixture was heated under refluxed for 2 h. After cooling to room temperature, the reaction mixture was concentrated under reduced pressure and purification of the residue by column chromatography (toluene/acetone, 5:1, *v/v*) on silica gel afforded **14** (25 mg, 78%) as a colorless oil; R_f 0.36 (toluene/acetone, 2:1, *v/v*); ^{1}H NMR (300 MHz, $CDCl_3$): δ = 7.46–7.09 (m, 5H, Ph), 6.18 (d, $J_{5,NH}$ = 8.7 Hz, 1H, NH), 5.92 (s, 1H, PhC*H*(OAc)CO), 4.80 (t, $J_{2,3}$ = 5.4 Hz, $J_{3,4}$ = 4.8 Hz, 1H, H-3), 4.61–4.44 (m, 3H, H-1, H-2, H-4), 2.13 (s, 3H, PhCH(CH_3CO)CO), 1.93 (m, 1H, H-5), 1.79 (s, 3H, CH_3CONH), 1.45–1.19 (m, 10H, C_6H_{10}); ^{13}C NMR (75 MHz, $CDCl_3$): δ = 170.5, 169.4, 167.9 (*C*=O), 133.3–128.1 (C_{arom}), 112.4 (C_6H_{10}), 77.7 (C-2), 77.1 (C-1), 74.6 (PhCH(OAc)CO), 74.4 (C-3), 50.4 (C-4), 34.5 (C-5), [35.8, 32.8, 24.9, 23.7, 23.3 (C_6H_{10})], 23.0 (CH_3CONH), 20.7 (PhCH(CH_3CO)CO); HRMS: *m/z*: found $[M+Na]^+$ 454.1858, $C_{23}H_{29}NO_7$ calcd for $[M+Na]^+$ 454.1862.

*(1R,2S,3R,4R,5R)-5-Aminocyclopentane-1,2,3,4-tetraol (**4a**)*: A suspension of **10** (40 mg, 0.11 mmol) and Pd/C (40 mg, 10%) in *tert*-butanol/H_2O/AcOH (5 mL, 40:1:1, *v/v/v*) was placed under an atmosphere of hydrogen. The reaction mixture was stirred at room temperature for 18 h, and then filtered through celite. The filtrate was concentrated to dryness. A solution of the residue in HCl (1 M) in H_2O/MeOH (8 mL, 1:1, *v/v*) was heated under refluxed for 2 h and then concentrated to dryness. Purification of the residue over Iatro beads (acetonitrile/AcOH/H_2O, 5:1:1, *v/v/v*) afforded **4a** (15 mg, quant.) as a white amorphous solid; ^{1}H NMR (300 MHz, D_2O): δ = 4.24 (dd, $J_{3,4}$ = 4.5 Hz, $J_{4,5}$ = 6.6 Hz, 1H, H-4), 4.08 (t, $J_{1,5}$ = 6.6 Hz, $J_{1,2}$ = 6.9 Hz, 1H, H-1), 4.02 (t, $J_{2,3}$ = 4.8 Hz, $J_{3,4}$ = 4.5 Hz, 1H, H-3), 3.80 (dd, $J_{1,2}$ = 6.9 Hz, $J_{2,3}$ = 4.8 Hz, 1H, H-2), 3.35 (t, $J_{1,5}$ = 6.6 Hz, $J_{4,5}$ = 6.6 Hz, 1H, H-5); ^{13}C NMR (75 MHz, D_2O): δ = 78.7 (C-3), 75.5 (C-2), 71.7 (C-4), 67.4 (C-1), 56.8 (C-5); HRMS: *m/z*: found $[M+H]^+$ 150.0776, $C_5H_{11}NO_4$ calcd for $[M+H]^+$ 150.0766.

*(1R,2R,3R,4S,5R)-4-Amino-5-methoxycyclopentane-1,2,3-triol (**5**)*: A suspension of **11** (38 mg, 0.10 mmol) in *tert*-butanol/H_2O/AcOH (5 mL, 40:1:1, *v/v/v*), Pd/C (35 mg, 10%) was placed under an atmosphere of hydrogen. The reaction mixture was stirred at room temperature for 18 h, and then filtered through celite. The filtrate was concentrated to dryness. A solution of the residue in HCl (1 M) in H_2O/MeOH (8 mL, 1:1, *v/v*) was heated under refluxed for 2 h and then concentrated to dryness. Purification of the residue over Iatro beads (acetonitrile/AcOH/H_2O, 5:1:1, *v/v/v*) afforded **5** (17 mg, quant.) as a white amorphous solid; ^{1}H NMR (300 MHz, D_2O): δ = 4.22 (dd, $J_{2,3}$ = 4.2 Hz, $J_{3,4}$ = 5.7 Hz, 1H, H-3), 4.02 (t, $J_{1,2}$ = 4.2 Hz, $J_{2,3}$ = 4.2 Hz, 1H, H-2), 3.95 (t, $J_{1,5}$ = 4.8 Hz, $J_{1,2}$ = 4.2 Hz, 1H, H-1), 3.83 (t, $J_{4,5}$ = 5.7 Hz, $J_{1,5}$ = 4.8 Hz, 1H, H-5), 3.45 (m, 1H, H-4); ^{13}C NMR (75 MHz, D_2O): δ = 88.8 (C-5), 74.4 (C-1), 72.3 (C-2), 68.4 (C-3), 58.1 (OCH_3), 55.3 (C-4); HRMS: *m/z*: found $[M+H]^+$ 164.0932, $C_6H_{13}NO_4$ calcd for $[M+H]^+$ 164.0923.

*(1S,2S,3R,4R)-4-Aminocyclopentane-1,2,3-triol (**3**)*: A solution of **14** (25 mg, 0.06 mmol) in HCl (1 M) in H_2O/MeOH (5 mL, 1:1, *v/v*) was heated under refluxed for 2 h and then concentrated to dryness. Purification of the residue over Iatro beads (*tert*-butanol/AcOH/H_2O, 4:1:1, *v/v*/v) afforded **3** (11 mg, quant.) as a white amorphous solid; ^{1}H NMR (500 MHz, D_2O): $\delta = 4.11–4.06$ (m, 2H, H-1, H-3), 3.91 (t, $J_{1,2} = 4.5$ Hz, $J_{2,3} = 4.0$ Hz, 1H, H-2), 3.58 (m, 1H, H-4), 2.46 (ddd, $J_{1,5} = 8.5$ Hz, $J_{4,5} = 7.5$ Hz, $J_{5,5'} = 15.0$ Hz, 1H, H-5), 1.69 (ddd, $J_{1,5'} = 5.0$ Hz, $J_{4,5'} = 6.0$ Hz, $J_{5,5'} = 15.0$ Hz, 1H, H-5′); ^{13}C NMR (75 MHz, D_2O): $\delta = 75.8$ (C-2), [72.4, 72.3 (C-1, C-3)], 53.4 (C-4), 37.0 (C-5); HRMS: *m/z*: found $[M+H]^+$ 134.0826, $C_6H_{13}NO_4$ calcd for $[M+H]^+$ 134.0817.

Enzymology: Inhibition constants were determined as detailed by Li et al.[36]

X-ray crystallography: Crystallization, data collection and refinement of the complexes were essentially as outlined in detail previously.[6,34] Graphics were generated with PyMOL.[37] The *Drosophila* Golgi α-mannosidase II (dGMII) was prepared as described previously.[30] Complexes of **2**, **4b** and **5** were prepared as cocrystals, while complexes with **3** and **4a** were prepared by soaking of phosphate washed crystals;[31] soak times were approximately 3 h.

For assessing the pH effect on mannostatin A binding, crystals were originally washed in phosphate buffered reservoir solution (pH 7) to remove the Tris from the active site, transferred briefly to reservoir buffers of appropriate pH (acetate, pH 3.8, MES pH 5.75 or CHES pH 9) followed by 30 min soaks with mannostatin A (1 mM) in reservoir buffer at the various pH values. Crystals were cryoprotected with increasing concentrations of MPD (up to 25%) at the various pH values and snap-frozen in liquid N_2.

Coordinates for protein complexes reported in this manuscript are deposited in the Protein Data Base with the ID codes: 3D4Y, 3D4Z, 3D50, 3D51 and 3D52.

Abbreviations: GMII: Golgi α1,3 α1,6-mannosidase II (E.C. 3.2.1.114); dGMII: catalytic domain of *Drosophila melanogaster* GMII; ABP: bacterial L-arabinose binding protein.

Acknowledgements

Funding was provided by National Institutes of Health, grant 5P41RR05351-18 (G.J.B), the Canadian Institutes of Health Research, grant MOP79312 (D.R.R), and the Mizutani Foundation, grant 080032 (D.R.R). This work is based upon research conducted at the Cornell High Energy Synchrotron Source (CHESS), which is supported by the National Science Foundation under award DMR-0225180, by using the Macromolecular Diffraction at CHESS (MacCHESS) facility, which is supported by an award from the National Institutes of Health, through its National Center for Research Resources (RR-01646).

Keywords: enzymes · Golgi mannosidase II · inhibitors · mannostatin A · thiomethyl group

[1] P. E. Goss, M. A. Baker, J. P. Carver, J. W. Dennis, *Clin. Cancer Res.* **1995**, *1*, 935–944.
[2] P. E. Goss, C. L. Reid, D. Bailey, J. W. Dennis, *Clin. Cancer Res.* **1997**, *3*, 1077–1086.
[3] N. Harpaz, H. Schachter, *J. Biol. Chem.* **1980**, *255*, 4894–4902.
[4] K. W. Moremen, O. Touster, P. W. Robbins, *J. Biol. Chem.* **1991**, *266*, 16876–16885.
[5] S. Numao, D. A. Kuntz, S. G. Withers, D. R. Rose, *J. Biol. Chem.* **2003**, *278*, 48074–48083.
[6] W. Zhong, D. A. Kuntz, B. Ernber, H. Singh, K. W. Moremen, D. R. Rose, G. J. Boons, *J. Am. Chem. Soc.* **2008**, *130*, 8975–8983.
[7] N. Shah, D. A. Kuntz, D. R. Rose, *Proc. Natl. Acad. Sci. USA* **2008**, *105*, 9570–9575.
[8] T. Aoyagi, T. Yamamoto, K. Kojiri, H. Morishima, M. Nagai, M. Hamada, T. Takeuchi, H. Umezawa, *J. Antibiot.* **1989**, *42*, 883–889.
[9] J. E. Tropea, G. P. Kaushal, I. Pastuszak, M. Mitchell, T. Aoyagi, R. J. Molyneux, A. D. Elbein, *Biochemistry* **1990**, *29*, 10062–10069.
[10] S. P. Kawatkar, D. A. Kuntz, R. J. Woods, D. R. Rose, G. J. Boons, *J. Am. Chem. Soc.* **2006**, *128*, 8310–8319.
[11] S. B. King, B. Ganem, *J Am Chem. Soc* **1994**, *116*, 562–570.
[12] S. Ogawa, T. Morikawa, *Bioorg. Med. Chem. Lett.* **1999**, *9*, 1499–1504.
[13] M. Kleban, P. Hilgers, J. N. Greul, R. D. Kugler, J. Li, S. Picasso, P. Vogel, V. Jager, *ChemBioChem* **2001**, *2*, 365–368.
[14] O. Boss, E. Leroy, A. Blaser, J. L. Reymond, *Org. Lett.* **2000**, *2*, 151–154.
[15] C. Uchida, H. Kimura, S. Ogawa, *Bioorg. Med. Chem.* **1997**, *5*, 921–939.
[16] F. Popowycz, S. Gerber-Lemaire, R. Demange, E. Rodriguez-Garcia, A. T. C. Asenjo, I. Robina, P. Vogel, *Bioorg. Med. Chem. Lett.* **2001**, *11*, 2489–2493.
[17] S. Ogawa, K. Washida, *Eur. J. Org. Chem.* **1998**, 1929–1934.
[18] C. Bournaud, D. Robic, M. Bonin, L. Micouin, *J. Org. Chem.* **2005**, *70*, 3316–3317.
[19] D. Pal, P. Chakrabarti, *J. Biomol. Struct. Dyn.* **1998**, *15*, 1059–1072.
[20] D. Pal, P. Chakrabarti, *J. Biomol. Struct. Dyn.* **2001**, *19*, 115–128.
[21] U. Samanta, D. Pal, P. Chakrabarti, *Proteins: Struct., Funct., Genet.* **2000**, *38*, 288–300.
[22] M. Iwaoka, S. Takemoto, M. Okada, S. Tomoda, *Bull. Chem. Soc. Jpn.* **2002**, *75*, 1611–1625.
[23] J. M. Holton, *J. Synchrotron Radiat.* **2007**, *14*, 51–72.
[24] W. P. Burmeister, *Acta Crystallogr., Sect. D: Biol. Crystallogr.* **2000**, *56*, 328–341.
[25] J. Yano, J. Kern, K. D. Irrgang, M. J. Latimer, U. Bergmann, P. Glatzel, Y. Pushkar, J. Biesiadka, B. Loll, K. Sauer, J. Messinger, A. Zouni, V. K. Yachandra, *Proc. Natl. Acad. Sci. USA* **2005**, *102*, 12047–12052.
[26] D. A. Kuntz, A. Ghavami, B. D. Johnston, B. M. Pinto, D. R. Rose, *Tetrahedron: Asymmetry* **2005**, *16*, 25–32.
[27] N. S. Kumar, D. A. Kuntz, X. Wen, B. M. Pinto, D. R. Rose, *Proteins Struct. Funct. Bioinf.* **2008**, *71*, 1484–1496.
[28] D. A. Kuntz, C. A. Tarling, S. G. Withers, D. R. Rose, *Biochemistry* **2008**, *74*, 10058–10068.
[29] F. A. Quiocho, D. K. Wilson, N. K. Vyas, *Nature* **1989**, *340*, 404–407.
[30] J. M. H. van den Elsen, D. A. Kuntz, D. R. Rose, *EMBO J.* **2001**, *20*, 3008–3017.
[31] N. Shah, D. A. Kuntz, D. R. Rose, *Biochemistry* **2003**, *42*, 13812–13816.
[32] W. Chen, D. A. Kuntz, T. Hamlet, L. Sim, D. R. Rose, M. B. Pinto, *Bioorg. Med. Chem.* **2006**, *14*, 8332–8340.
[33] D. A. Kuntz, H. Liu, M. Bols, D. R. Rose, *Biocatal. Biotransform.* **2006**, *24*, 55–61.
[34] H. Fiaux, D. A. Kuntz, R. C. Janzer, S. Gerber-Lemaire, D. R. Rose, L. Juillerat-Jeannere, *Bioorg. Med. Chem.* **2008**, *16*, 7337–7346.
[35] P. Englebienne, H. Fiaux, D. A. Kuntz, C. R. Corbeil, S. Gerber-Lemaire, D. R. Rose, N. Moitessier, *Proteins Struct. Funct. Bioinf.* **2007**, *69*, 160–176.
[36] B. Li, S. P. Kawatkar, S. George, H. Strachan, R. J. Woods, A. Siriwardena, K. W. Moremen, G. J. Boons, *ChemBioChem* **2004**, *5*, 1220–1227.
[37] W. L. DeLano, *The PyMol Molecular Graphics System*, DeLano Scientific, Palo Alto, CA, **2008**.
[38] A. T. Brünger, P. D. Adams, G. M. Clore, W. L. DeLano, P. Gros, R. W. Grosse-Kunstleve, J.-S. Jiang, J. Kuszewski, M. Nilges, N. S. Pannu, R. J. Read, L. M. Rice, T. Simonson, G. L. Warren, *Acta Crystallogr. Sect. D* **1998**, *54*, 905–921.
[39] P. Emsley, K. Cowtan, *Acta Crystallogr. Sect. D* **2004**, *60*, 2126–2132.

Received: August 8, 2008
Published online on December 19, 2008

